Waste Management 95 (2019) 289–297

Contents lists available at ScienceDirect

Waste Management

journal homepage: www.elsevier.com/locate/wasman

Impacts of iron oxide nanoparticles on organic matter degradation and microbial enzyme activities during agricultural waste composting

Lihua Zhang [a,b,1], Yuan Zhu [a,b,1], Jiachao Zhang [c,1], Guangming Zeng [a,b,*], Haoran Dong [a,b,*], Weicheng Cao [a,b], Wei Fang [a,b], Yujun Cheng [a,b], Yaoyao Wang [a,b], Qin Ning [a,b]

[a] College of Environmental Science and Engineering, Hunan University, Changsha 410082, PR China
[b] Key Laboratory of Environmental Biology and Pollution Control, Hunan University, Ministry of Education, Changsha 410082, PR China
[c] College of Resources and Environment, Hunan Agricultural University, Changsha 410128, PR China

ARTICLE INFO

Article history:
Received 9 January 2019
Revised 30 May 2019
Accepted 13 June 2019

Keywords:
Composting
Iron oxide nanoparticles
Organic matter
Enzyme activity
Redundancy analysis

ABSTRACT

The effects of iron oxide nanoparticles (IONPs, including Fe_2O_3 NPs and Fe_3O_4 NPs) on composting were investigated through evaluating their influences on organic matter (OM) degradation, dehydrogenase (DHA) and urease (UA) activities, and quality of the final compost product. Results showed that composting amended with Fe_2O_3 NPs was more effective to facilitate OM degradation. At the end of composting, the total OM loss in T-C, T-Fe_2O_3 NPs and T-Fe_3O_4 NPs was 66.19%, 75.53% and 61.31%, respectively. DHA and UA were also improved on the whole by the amendment of IONPs, especially Fe_2O_3 NPs. Although relationships between enzyme activities and environmental variables were changed by different treatments, temperature was the most influential to variations of both DHA and UA in all treatments, which independently explained 75.1%, 34.7% and 38.4% of variations in the two enzyme activities in T-C, T-Fe_2O_3 NPs and T-Fe_3O_4 NPs, respectively. Compared with DHA, UA was more closely related to the environmental parameters. The germination index in T-C, T-Fe_2O_3 NPs and T-Fe_3O_4 NPs was 134.49%, 153.64% and 146.76%, and the average shoot length was 3.16, 3.87 and 3.45 cm, respectively, indicating that amendment of IONPs, especially Fe_2O_3 NPs, could promote seed germination and seedling growth. Therefore, composting amended with IONPs was a feasible and promising method to improve composting performance, enzyme activities as well as quality of the final compost product.

1. Introduction

As one of the largest agricultural countries, China has produced more and more crop straws in recent years which are regarded as waste materials. According to Ministry of Agriculture of China (MOA, 2011), the annual output of straw residues in China was more than 600 million tons, ranking first in the world, and rice straw accounted for the largest proportion of 32.3%. When it came to 2015, the total yield exceeded 1.11 billion tons according to National Bureau of Statistics of China (NBS, 2016). Traditionally, most of these straws are burned on-site, not only leading to severe air pollution and greenhouse gas emission, but also contributing to soil fertility degradation (Gong et al., 2009; Huang et al., 2018). Since the crop straw is rich of nutrient elements and organic matters (OM), exploring an appropriate methodology to recycle it is a key way for sustainable crop production.

Composting has been widely recommended as an eco-friendly, economical and practical way to recycle agricultural waste (Zeng et al., 2018; Zhang et al., 2018b). During the composting process, agricultural waste can be bio-decomposed into stable humus-like substances and pathogenic microorganisms can also be eliminated, thereby recycled as environmentally friendly soil conditioner, fertilizer and remediation agent (Zhang et al., 2015). The readily available fractions of OM in agricultural straw can be immediately utilized by composting microbes, while polymeric organic compounds are dependent on the enzymatic activities to be degraded into directly available carbon and nitrogen sources (Jurado et al., 2015; He et al., 2018a). Among the polymers, lignin and cellulose are the main components and the most difficult to be degraded, thus inhibiting the composting process and reducing the final compost quality. Many researches have tried to improve the OM degradation during composting by various methods, such as inoculation with exogenous microorganisms (Jurado et al., 2015; Yang et al.,

* Corresponding authors at: College of Environmental Science and Engineering, Hunan University, Changsha 410082, PR China.
E-mail addresses: zgming@hnu.edu.cn (G. Zeng), dongh@hnu.edu.cn (H. Dong).
[1] These authors contributed equally to this paper.

https://doi.org/10.1016/j.wasman.2019.06.025
0956-053X/

2018a), or amendment of biochar, zeolite, etc. (Hagemann et al., 2018; Yi et al., 2018).

The unique physical, electronic, optical, and biological properties of engineered nanoparticles (ENPs) have resulted in a rapid increase in their application, including architecture, aerospace and airplanes, computer memory, catalysts, chemicals, environmental protection, etc. (Xu et al., 2012; Wang et al., 2018). With the production and application of ENPs rapidly expanding, their environmental impacts are attracting more and more attentions. Iron is an essential nutrient for most of microorganisms and plants since it plays a critical role in cell growth. It also acts as a cofactor for many kinds of enzymes and is demanded for many biochemical reactions, such as respiration, nitrogen fixation and DNA synthesis, etc. (He et al., 2011). A previous study suggested that Fe_2O_3 NPs could promote the growth of plant, such as mung bean (*Vigna radiata*) (Ren et al., 2011). It was also reported that dehydrogenase (DHA) and urease activity (UA) in soil positively responded to the treatments of iron oxide nanoparticles (IONPs, including Fe_2O_3 and Fe_3O_4 NPs), in which Fe_2O_3 NPs exhibited more significant effects, as the changes of microbial community caused by IONPs could induce variations in enzyme activities (He et al., 2011; He et al., 2018b). DHA and UA are real reflections of performance of biological process during composting in terms of OM degradation and nitrogen cycle, and also provide information about maturity of the compost product (Ye et al., 2017a; Ren et al., 2018b). However, as yet, few researches are concerned about the enzyme activities and OM degradation during composting process with the amendment of IONPs. Moreover, most of previous studies about nanomaterials in composting systems were mainly focused on Ag or Ag-based NPs (Gitipour et al., 2013; Stamou et al., 2016), so, additional kinds of NPs are also worth studying.

Thus, the present study aimed to evaluate the OM degradation and enzyme activities during composting which were amended with two types of IONPs (Fe_2O_3 and Fe_3O_4 NPs) to improve and promote the process performance. Additionally, as the enzyme activities may be sensitive to the changes of environment, it is also necessary to evaluate the relationships between enzyme activities and composting parameters, and identify the driving factors. The results of this study will provide a valuable basis for promoting the application of nanotechnology in the field of composting.

2. Materials and methods

2.1. IONPs preparation

Fe_2O_3 NPs was synthesized by forced hydrolysis of ferric nitrate solution according to Barton et al. (2011). Briefly, 60 mL of 1 M ferric nitrate solution was dripped into 750 mL of boiling ultrapure water. The boil was maintained using a hot plate with vigorous stirring during the whole process. After completion of ferric nitrate addition, the solution was removed from heat and cooled for 24 h. The synthetic NPs were purified with dialysis bag and stored at 4 °C in dark.

Chemical coprecipitation method was used for preparation of Fe_3O_4 NPs according to Yang et al. (2012) with a little modification. A mixture of iron solution was prepared by dissolving $FeCl_3{\cdot}6H_2O$ (12.3 g) and $FeSO_4{\cdot}7H_2O$ (8.5 g) in 200 mL of ultrapure water, which was then heated to 90 °C with constant stirring in a 500 mL round-bottom flask equipped with a reflux condenser. Then, 25% of ammonium hydroxide solution (30 mL) was added into the solution rapidly and sequentially and stirred at 90 °C for 1 h. Finally, the solid products (Fe_3O_4 NPs) were rinsed several times with ultrapure water and were ready for use.

Particle size distribution and morphology of the two NPs were measured via transmission electron microscopy (TEM) using a field-emission transmission electron microscope (Tecnai G2 F20, FEI). Results showed that the average diameter of Fe_2O_3 NPs and Fe_3O_4 NPs was 8.7 and 15.6 nm, respectively, and the shape was globular (see Fig. S1 in Supplementary material).

2.2. Composting raw materials preparation

The components of raw materials were prepared referring to our previous studies (Zhang et al., 2017; Zhou et al., 2018). Rice straw, used as the typical agricultural waste which is difficult to be degraded, was obtained from a suburb of Changsha, China. Vegetable waste was collected from a vegetable market and used to speed up the beginning of composting. Both rice straw and vegetable waste were air-dried and cut into about 15 mm length. The soil, which was added to enrich microbial populations and offer some necessary nutrients, was dug from Yuelu Mountain of Changsha, China, and sieved through 60-mesh screen to remove the coarse plant debris. Bran, purchased from a farm of Henan province, China, was added to adjust the initial carbon to nitrogen ratio (C/N) after air-dried. Characterizations of raw materials were presented in Table S1 of Supplementary material.

2.3. Composting and sampling

60 days of lab-scale composting experiments with different treatments were conducted in reactors with 65 L of capacity. Rice straw, soil, vegetable and bran were homogenized at a weight ratio of 30:27:8:5 to obtain an initial C/N ratio of about 30. The control treated without any IONPs was marked as T-C, and treatments with Fe_2O_3 NPs and Fe_3O_4 NPs at a concentration of 10 mg/kg compost were named as T- Fe_2O_3 NPs and T- Fe_3O_4 NPs, respectively. Initial moisture content was adjusted to about 55%. To ensure sufficient aeration, the composting piles were manually turned daily in the beginning 14 days and on each sampling day afterwards. Three subsamples were collected and homogenized on day 0, 3, 5, 7, 17, 29, 43, 60. These mixed samples were then stored at 4 °C for further physicochemical and enzymatic analyses.

2.4. Physicochemical determination

The pile temperatures were determined using ordinary thermometer from three different positions of the piles, and the ambient temperature was also recorded. Samples for pH determination were shaken in ultrapure water at a ratio of 1:10 (weight/volume, w/v) and then the suspension was collected using ordinary filter paper. NH_4^+-N and NO_3^--N were determined using flow injection analysis (AA3, Germany) after being extracted by shaking the samples with 2 M KCl at a ratio of 1:50 (w/v) under 150 rpm for 1 h. The OM and ash content were determined using dry combustion in a muffle furnace at 550 °C for 6 h after the samples were firstly dried at 105 °C for 24 h and ground. The content of total organic carbon (TOC) and OM loss were calculated on basis of ash content with reference to the following equations, respectively (Zhang et al., 2017; Qin et al., 2018):

$$\%\mathrm{TOC} = (100 - \%\mathrm{ash})/1.8 \quad (1)$$

$$\%\mathrm{OM\ loss} = 100 - 100[X_1(100 - X_n)]/[X_n(100 - X_1)] \quad (2)$$

where X_1 represented the initial ash content and X_n was the ash content on each corresponding day. Water soluble carbon (WSC) was determined using Total Organic Carbon Analyzer (TOC-5000A, Shimadzu, Japan). Samples submerged in ultrapure water at a ratio of 1:10 (w/v) were shaken at 200 rpm for 40 min. Then, the supernatant was collected via filtering using ordinary filter paper and then centrifuged at 12,000 rpm for 10 min, and further cleared using 0.45 μm membrane filter. Total nitrogen (TN) was determined

by elemental analyzer (Elementar, Vario Max CN, Germany). C/N equals to the ratio of TOC and TN.

The germination index (GI) was tested using radish seed according to Wu et al. (2019) with a little modification. Firstly, fresh compost was shaken with ultrapure water (1:10, w/v) for 1 h and the mixture was filtered to collect the aqueous extracts. Secondly, twenty seeds were placed into 9 cm Petri dishes which were lined with Whatman filter paper and contained 10 mL of extracts. Ultrapure water was used as control. Then the above Petri dishes were incubated at 25 °C in dark for 3 days. Finally, seed germination, root length, shoot length were determined, and relative seed germination (SG), relative root elongation (RE) and germination index (GI) were calculated according to Wu et al. (2019).

2.5. Enzyme activity determination

DHA was analyzed according to the transformation of 1,3,5-triphenyltetrazolium chloride (TTC) to triphenylformazan (TPF) by method of Liu et al. (2014). Firstly, 2 g of fresh compost was mixed with 10 mL of 0.5% TTC solution. Then, the mixture was incubated at 37 °C for 8 h in dark. The blank control was processed by replacing TTC with the same volume of ultrapure water. After incubation, the formed TPF was extracted by shaking the mixture with 100 mL of methanol at 300 rpm for 1 h. The supernatant was cleared and collected through centrifugation. Finally, the concentration of TPF was determined using spectrophotometry at 485 nm and the results were reported as mg TPF g^{-1} dry compost $(8\ h)^{-1}$.

UA was calculated based on the NH_4^+-N produced after incubation of compost samples with urea solution as described by Gutiérrez et al. (2010). 10 mL of 40 mM aqueous urea solution was added to 1 g of compost, and the control was added with 10 mL of ultrapure water. After incubation at 37 °C for 6 h, 10 mL of ultrapure water (control: 10 mL of 40 mM urea solution) and 50 mL of a KCl-HCl (1 M KCl; 0.01 M HCl) were added to extract the produced NH_4^+-N by shaking the mixture at 150 rpm for 40 min. The suspension for NH_4^+-N determination by spectrophotometry at 490 nm was filtered successively using filter paper and 0.45 μm membrane filter. The enzyme activity was expressed as mg NH_4^+-N g^{-1} dry compost $(6\ h)^{-1}$.

2.6. Statistical analysis

The first-order kinetic model was used to assess OM evolution and loss during composting via fitting the data of OM content or OM loss as a function of composting time which were expressed as follows (He et al., 2018c; Xiong et al., 2018):

$$\text{OM}\ (\%) = A \times e^{-kt} \quad (3)$$

$$\text{OM loss}\ (\%) = A(1 - e^{-kt}) \quad (4)$$

In which A was the initial OM content (%) for Eq. (3) or the maximum OM loss (%) for Eq. (4), k was the rate constant (day^{-1}) and t was the composting time in days. The residual mean square (RMS) and F-values were used to verify the significance of the curve fitting.

Mean values with standard deviation ($n = 3$) were presented on basis of dry weight (DW) for all determinations. The significance of difference between mean values of different samples was assessed by one–way analysis of variance (ANOVA) using SPSS 19.0 which was based on a 95% confidence level. Multivariate relationships between enzyme activities and physicochemical parameters were tested with Canoco 4.5 as described in our previous study (Zhang et al., 2018b). Pearson correlations between enzyme activities and environmental variables were evaluated using SPSS 19.0.

3. Results and discussion

3.1. Changes of physicochemical parameters

Temperature is an important parameter affecting the performance of organic solid waste aerobic composting and can reflect the biological activity in composting system (Ren et al., 2018a). As shown in Fig. 1A, the maximum and minimum ambient temperature during the whole composting process was 28 and 17 °C, respectively. The temperatures in all the three treatments showed a rapid increase in the first 6 days, and the maximum value was greater than 65 °C in each composting treatment. This rapid increase of temperature might be attributed to the decomposition of easily degradable organic matters by microorganisms which released a lot of heat. Though the maximum temperatures in all treatments were not significantly different, the duration of temperature above 55 °C in IONPs treatments was longer than that in the control. With the degradation of simple organic matters, the temperature in all treatments began to decrease until the end of composting process. Intriguingly, the temperature in T-C was significant higher ($P < 0.05$) than IONPs treatments during day 20 to 40, especially T-Fe_2O_3 NPs, this might be caused by the more slowly degradation of available OM during earlier stage in T-C, which consequently maintained higher temperature in T-C during this phase.

In addition, the pH of the three composting treatments experienced the similar pattern, showing significant fluctuation in the first 17 days due to the intensive activities of microorganisms during this stage, and then it changed slowly (Fig. 1B). The final pH of all treatments maintained as 8–8.2, indicating that the final compost reached maturation (Zhang et al., 2018a). The higher pH in IONPs treatments during the 10th to 43rd day might be attributed to higher NH_4^+-N in the two treatments (Fig. 1C). As shown in Fig. 1C, the NH_4^+-N contents in all treatments reached peak value on the 5th day, which might be caused by the ammonification of organic N, and then decreased because of nitrification, NH_3 emission, etc. At the end of composting, the NH_4^+-N in T-Fe_2O_3 NPs was significant higher than that of T-C, while the NO_3^--N in T-Fe_2O_3 NPs was significant lower than T-C (Fig. 1D). The final mineral nitrogen in T-C, T-Fe_2O_3 NPs and T-Fe_3O_4 NPs was 0.78, 0.92 and 0.78 g/kg DW compost, respectively, indicating that Fe_2O_3 NPs was more beneficial to improve the nitrogen utilization efficiency of final compost product.

3.2. Changes of organic matter

Organic matter (OM) is an important indicator to evaluate the transformation and mineralization of organic nutrients during composting process (Chan et al., 2016; Yang et al., 2018b). As shown in Fig. 2A, OM content was constantly decreased in all treatments, which was generally attributed to the utilization of OM and emission of CO_2 by microorganisms (Awasthi et al., 2016b; Tang et al., 2018). Overall speaking, the OM was decreased from 64.38, 63.64 and 61.95% to 37.93, 29.99 and 38.65% in T-C, T-Fe_2O_3 NPs and T-Fe_3O_4 NPs, respectively. The OM was most intensively mineralized within the first 17 days in all treatments, which resulted in higher temperatures. Afterwards, it was decreased more slowly as the consumption of easily degradable OM and the remaining component was recalcitrant to be degraded. The OM loss rates were 51.29, 52.82 and 52.29% within the first 17 days, respectively, accounting for 77.49, 69.93 and 85.29% of the total OM loss. The higher OM loss and lower proportion of OM loss in the first 17 days to total OM loss in T-Fe_2O_3 NPs indicated that more OM was degraded not only in the first 17 days of composting but also afterwards, suggesting that the amendment of Fe_2O_3 NPs was beneficial

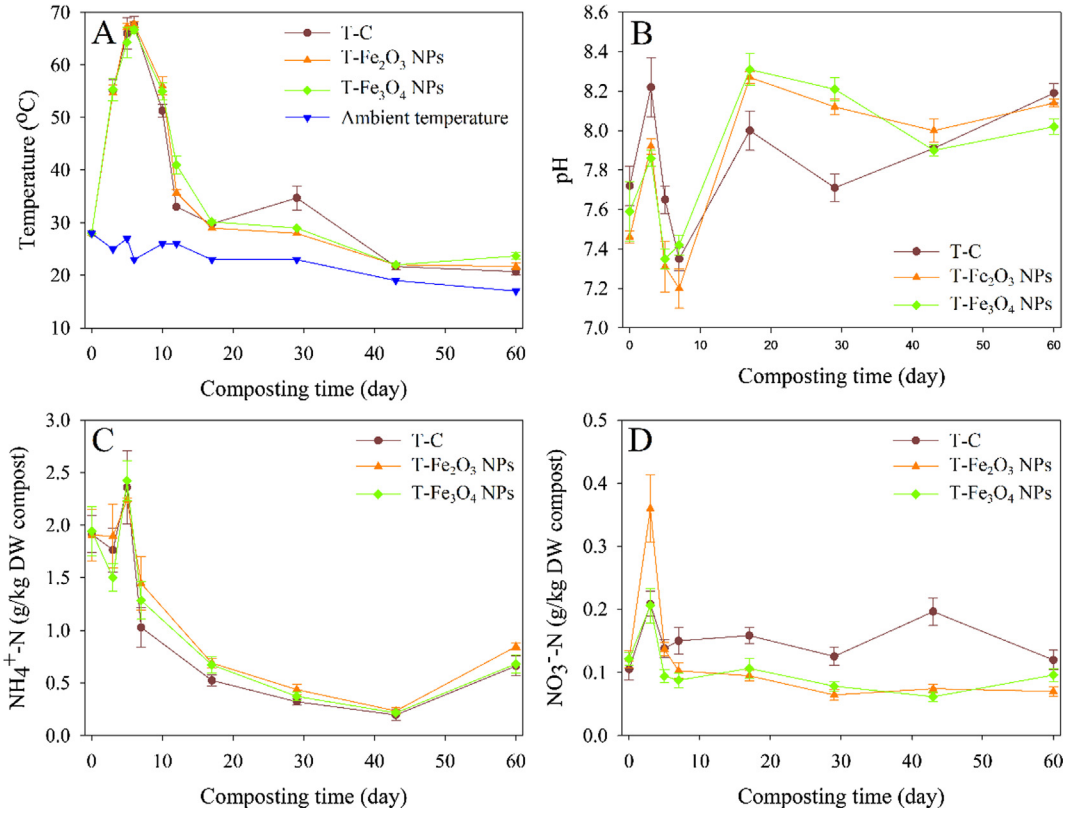

Fig. 1. Changes of (A) temperature; (B) pH; (C) NH_4^+-N and (D) NO_3^--N during composting. Mean values were shown and the error bars represented the standard deviations (n = 3).

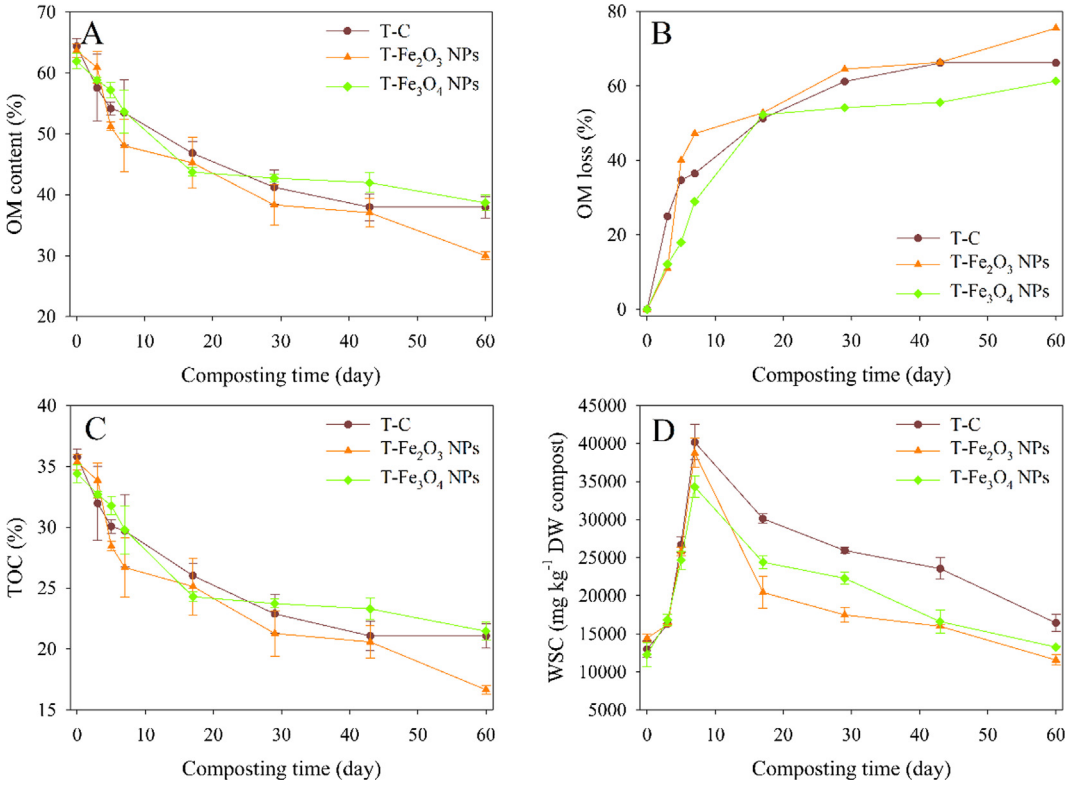

Fig. 2. Temporal courses of (A) organic matter (OM) degradation; (B) OM loss; (C) TOC, total organic carbon; (D) WSC, water soluble carbon during composting process. T-C: treatment without Fe_2O_3 NPs or Fe_3O_4 NPs as control; T- Fe_2O_3 NPs: treatment with Fe_2O_3 NPs; T- Fe_3O_4 NPs: treatment with Fe_3O_4 NPs. Data were calculated on a basis of dry weight compost. Mean values were shown and the error bars represented the standard deviations (n = 3).

to the degradation of recalcitrant OM. At the end of composting, the total OM loss in T-Fe_2O_3 NPs was significant higher than other two treatments with values of 66.19, 75.53 and 61.31% in T-C, T-Fe_2O_3 NPs and T-Fe_3O_4 NPs (Fig. 2B), respectively, and this was confirmed by the ANOVA test ($P < 0.001$).

To assess the organic biological degradation, the kinetics of OM degradation and loss were calculated. In all treatments, the OM evolution and loss profiles followed first-order kinetics along with the proceeding of composting. The parameters obtained from curve fitting of experimental data showed that all OM evolution and loss kinetics well fitted with the equations ($P < 0.05$) (Table 1). The rates of OM evolution and loss in T-Fe_2O_3 NPs were more rapid than T-C and T-Fe_3O_4 NPs, as shown by the higher k value. Greater OM loss was also detected in T-Fe_2O_3 NPs (Fig. 2B). However, Ben-Moshe et al. (2013) suggested that OM in soil was not changed with the addition of nanoparticles, and the underlying explanation was that the given experimental condition (i.e., short exposure time) did not support complete mineralization of OM. The conditions of composting in present study were supportive of microbial activities to degrade OM and thus caused differences in the three treatments.

The changes of TOC during composting process were presented in Fig. 2C. Generally, TOC contents decreased during the whole process of composting. More rapid loss of TOC contents during the first 17 days might be attributable to the utilization of easily degradable OM by microorganisms. Moreover, Awasthi et al (2016b) demonstrated that during the early phase of composting, a part of organic carbon in the compost is transformed to H_2O, CO_2 and energy, while the rest is continuously converted to more stable humus like substances. As shown in Fig. 2C, the TOC content in T-Fe_2O_3 NPs was relatively lower than the other two treatments on the whole during composting. At the end of composting, the TOC in T-Fe_2O_3 NPs was significantly lower than T-C and T-Fe_3O_4 NPs which was verified by the ANOVA results ($P < 0.001$). There were no significant differences in the TOC content as well as OM between T-C and T-Fe_3O_4 NPs ($P > 0.05$) in the end, since the positive effect of iron in Fe_3O_4 NPs as a nutrient might be impaired by the release of Fe^{2+} which could generate reactive oxygen species (ROS) (Auffan et al., 2008). The final TOC contents were 21.1%, 16.7% and 21.5%, and the TOC reduction compared with initial contents were observed with 41.1%, 52.9% and 37.6% in T-C, T-Fe_2O_3 NPs and T-Fe_3O_4 NPs, respectively.

WSC is always used as one of the most biologically active parameters to evaluate the compost stability. It can be easily and directly utilized or degraded by microorganisms, as it mainly consists of low-molecular weight organic acids, sugars, phenolic substances, amino acids, hemicellulose and other easily biodegradable compounds (Zhang et al., 2018b; Ye et al., 2017b). In this study, the WSC concentration in all treatments increased rapidly within the early 7 days (Fig. 2D), because the production of WSC by solubilization of some simple organic matters or by microbial activities and growth was greater than their consumption and degradation by microorganisms (Zhang et al., 2017). Afterwards, the WSC showed constant drop until the end of composting. The final WSC in T-C was significantly higher than that in T-Fe_2O_3 NPs and T-Fe_3O_4 NPs ($P < 0.01$), indicating that the further degradation or utilization of WSC in T-C was not greater than the other two treatments. As shown in Fig. 2A and 2D, both OM and WSC degradation in T-Fe_2O_3 NPs were greater than T-Fe_3O_4 NPs, indicating that the amendment of Fe_2O_3 NPs was more effective to improve the composting performance.

3.3. Enzyme activities

Dehydrogenase is an intracellular enzyme that catalyzes metabolic reactions for OM degradation to provide ATP. It has been confirmed that DHA can reflect the rate of biochemical reaction during composting and has been generally regarded as a reliable indicator for overall microbial activity in the composting system because it directly participates in the respiratory chain (Li et al., 2015). The dynamics of DHA in the three treatments were shown in Fig. 3A. It increased rapidly in all treatments during the early stage of composting until the maximum value was achieved in thermophilic phases, which was attributed to the oxidation of easily degradable OM catalyzed by the enzyme (Li et al., 2015), and then decreased until the end of composting. Similar observations were also reported by a previous study (Nikaeen et al., 2015) that found DHA reached the maximum in the initial stage and then decreased along with the composting process. Maximum DHA occurred on day 7 with values of 9.15, 11.34, 10.38 mg TPF g^{-1} dry compost $(8\ h)^{-1}$ in T-C, T-Fe_2O_3 and T-Fe_3O_4 NPs, respectively. As shown in Fig. 3A, DHA was higher in T-Fe_2O_3 and T-Fe_3O_4 NPs than the control on the whole, especially in the treatment with addition of Fe_2O_3 NPs during the 3rd to 17th day ($P < 0.05$), indicating that the addition of IONPs especially Fe_2O_3 NPs facilitated DHA and rates of biochemical reactions, and this corresponded to the greater degradation of OM and WSC in T-Fe_2O_3 NPs which were shown in Fig. 2A and 2D.

Urease, as an intracellular enzyme, can catalyze the transformation of amides into ammonium. Its activity has been considered as an enzymatic indicator of N mineralization (Wong et al., 2000). Similar to DHA, the UA in all treatments increased rapidly in the first 7 days, and then decreased until the end of composting (Fig. 3B), which was also observed in other previous study (Li et al., 2015). The production and accumulation of substrates related to nitrogen by other enzymatic activities might be the possible reason for the increase of UA, while the decrease of UA might be caused by the depletion of readily biodegradable OM which supports microbial activity (Sudkolai et al., 2017; Ren et al., 2018c). Compared with T-C, the treatments with IONPs enhanced

Table 1
Parameter values of the first-order equation kinetics obtained from curve fitting of OM degradation and OM loss.

Treatment	A (%)	k	RMS	F
OM degradation				
T-C	58.69 (2.01)	0.0095 (0.0016)	13.76	42.38
T-Fe_2O_3 NPs	58.39 (2.43)	0.0123 (0.0021)	19.32	43.47
T-Fe_3O_4 NPs	58.40 (2.08)	0.0085 (0.0016)	14.94	32.24
OM loss				
T-C	63.82 (2.20)	0.1335 (0.0157)	13.85	265.44
T-Fe_2O_3 NPs	68.51 (4.53)	0.1379 (0.0286)	57.04	82.38
T-Fe_3O_4 NPs	59.87 (2.27)	0.0906 (0.0108)	10.30	368.43

A: the initial organic matter (OM) content (%) for OM degradation kinetic or the maximum OM loss (%) for OM loss kinetic. k: rate constant (d^{-1}). RMS: residual mean square. F: factor significant at $P < 0.05$. The value in brackets: standard deviation. T-C: treatment without Fe_2O_3 NPs or Fe_3O_4 NPs as control; T- Fe_2O_3 NPs: treatment with Fe_2O_3 NPs; T-Fe_3O_4 NPs: treatment with Fe_3O_4 NPs.

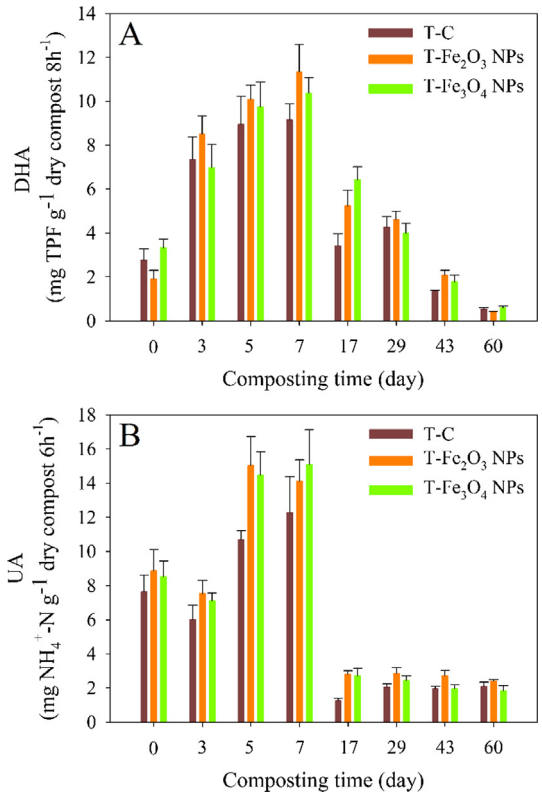

Fig. 3. Evolutions of enzyme activities (A) dehydrogenase activity (DHA); (B) urease activity (UA) during composting process. T-C: treatment without Fe_2O_3 NPs or Fe_3O_4 NPs as control; T- Fe_2O_3 NPs: treatment with Fe_2O_3 NPs; T- Fe_3O_4 NPs: treatment with Fe_3O_4 NPs. Data were calculated on a basis of dry weight compost. Mean values were shown and the error bars represented the standard deviations ($n = 3$).

the average UA in order of T-Fe_2O_3 NPs > T-Fe_3O_4 NPs, as well as DHA. Similar results were reported by He et al. (2011) who found that IONPs had positive effects on the soil UA and DHA, and they also found that Fe_2O_3 NPs addition had greater impacts on the enzyme activities.

It has been suggested that iron-based NPs are toxic because of the reactive oxygen species (ROS) (Auffan et al., 2008). Therefore, the positive effect of Fe_3O_4 NPs as an iron nutrient may be counteracted by the release of Fe^{2+}, resulting in a weaker improvement of microbial activity, while Fe_2O_3 NPs consist of fully oxidized crystals which are very stable in environment, thus showing a lower capacity to generate ROS and inducing greater improvement of microbial activity (He et al., 2011). Overall, the amendment of IONPs, especially Fe_2O_3 NPs, could enhance the enzyme activities and promote the OM degradation in this study.

3.4. Relationships between physicochemical parameters and enzyme activities

According to the results of detrended correspondence analysis (DCA), the length of the first axis in all treatments was less than 3, which indicated linear relationships between enzyme activities and environmental variables during composting. Therefore, RDA was performed to evaluate the multivariate relationship between physico-chemical parameters and enzyme activities. Totally, eight environmental variables were selected in RDA model, including temperature, pH, C/N, TOC, WSC, NH_4^+-N, NO_3^--N and TN. In addition, Pearson correlations were conducted to support these analyses. To identify the driving factors of enzyme activities, manual forward selection was performed. Accordingly, temperature was the most influential factor ($P < 0.01$) in all treatments, and it was the only significant factor in T-C. Another driving factor in T-Fe_2O_3 NPs was pH ($P < 0.05$) and that in T-Fe_3O_4 NPs was WSC ($P < 0.05$). Partial RDA showed that temperature solely explained 75.1% ($P = 0.002$), 34.7% ($P = 0.016$) and 38.4% ($P = 0.044$) of the variation in enzyme activities in T-C, T-Fe_2O_3 NPs and T-Fe_3O_4 NPs, respectively (Table 2). The importance of temperature fluctuations for the evolution of enzyme activities has been highlighted by a previous study (Wang et al., 2011). In agreement, it was also found that both temperature and DHA activity showed a rapid increase during the early days of composting (Awasthi et al., 2018), indicating impacts on enzyme activities by temperature. Additionally, as an important parameter during composting, pH significantly accounted for 11% ($P = 0.05$) of the variation in enzyme activities in T-Fe_2O_3 NPs. The shared contribution of temperature and pH was 40.1%, indicating that the strong intercorrelation of the two factors also contributed to the changes of enzyme activities. These were also supported by the Pearson correlation between environmental variables in which temperature and pH were closely correlated with each other ($P < 0.05$) (see Table S3 of Supplementary materials). For T-Fe_3O_4, WSC, another significant explanatory variable tested by manual forward selection, solely explained 4.1% of the variation in enzyme activities, which was not significant ($P = 0.512$), while the total explanation of temperature and WSC was 76.3% ($P = 0.01$) (Table 2). This suggested that WSC contributed to the changes of enzyme activities mainly via cooperating with temperature (see Table S3 of Supplementary materials). However, these results did not imply that other environmental variables were not influential to the changes of enzyme activities, it was only deduced that these parameters contributed to the variations of enzyme activities mainly through the intercorrelation with other significant factors, as proved by Pearson correlation analysis between different variables (see Tables S2–S4 of Supplementary materials).

To further evaluate the relationships between enzyme activities and environmental variables, ordination triplots were created. The length and orientation of arrows represent the importance of

Table 2
Partial RDA results indicating the influence of the significant variables on enzyme activities.

Treatments	Variables tested in model	Eigenvalues	Sole explanation (%)	*F* value	*P* value
T-C	Temperature	0.751	75.1	18.087	0.002
T-Fe_2O_3 NPs	Temperature	0.347	34.7	12.242	0.016
	pH	0.110	11.0	3.896	0.050
	Together	0.858	85.8	15.150	0.002
T-Fe_3O_4 NPs	Temperature	0.384	38.4	8.090	0.044
	WSC	0.041	4.1	0.865	0.512
	Together	0.763	76.3	8.046	0.010

WSC: water soluble carbon; T-C: treatment without Fe_2O_3 NPs or Fe_3O_4 NPs as control; T- Fe_2O_3 NPs: treatment with Fe_2O_3 NPs; T- Fe_3O_4 NPs: treatment with Fe_3O_4 NPs.

parameters and associations between axis and parameters, respectively. Moreover, the angles between two parameters <90° reflect positive relationships, while that >90° reflect negative relationships. As shown in Fig. 4, the enzyme activities were negatively correlated with pH and TN, and shared positive relationship with other parameters in all treatments except weak negative correlations between NO_3^--N and UA in T-C. Longer arrow line of temperature, NH_4^+-N and TN indicated that these parameters played more important roles in explaining variations of enzyme activities in T-C (Fig. 4A). According to Pearson correlation (Table 3), both DHA and UA were positively correlated with temperature in all treatments ($P < 0.01$). This finding was in accordance with a previous study which found that DHA increased in the thermophilic stage and then rapidly decreased when the temperature dropped (Wang et al., 2011). Moreover, there was a significant ($P < 0.05$) positive relationship between UA and NH_4^+-N, and negative correlation with TN in T-C (Table 3). From Fig. 4B, temperature, pH, WSC and NH_4^+-N played relatively more important roles in variations of enzyme activities than other parameters, as supported by Table 3 showing an extremely significant negative correlation ($P < 0.01$) between UA and pH, extremely significant positive correlation between the enzyme activities and temperature ($P < 0.01$), and significant positive correlation between WSC, NH_4^+-N and enzyme activities ($P < 0.05$) in T-Fe_2O_3 NPs. A previous study also reported that the UA was negatively influenced by pH (Xie et al., 2017). pH not only has an influence on the decomposition and mineralization of organic macromolecules, species and activities of microorganisms, but also directly affects the rate of enzymes involved in biochemical processes (Dick et al., 2000; Lai et al., 2016). As for T-Fe_3O_4 NPs which was shown in Fig. 4C, the lengths of temperature, pH, C/N, TOC, WSC, NH_4^+-N and TN were longer, in which DHA was significantly correlated with temperature, C/N, WSC and TN, and UA shared significant correlation with temperature, pH, C/N, TOC and NH_4^+-N ($P < 0.05$) (Table 3). In T-Fe_2O_3 NPs and T-Fe_3O_4 NPs, WSC played an important role as well, similar with a previous study (Calvarro et al., 2014). As implied by Pearson correlation, UA was more closely related to environmental factors than DHA in all treatments. The different relationships between enzyme activities and environmental variables in three treatments suggested that the amendment of IONPs changed their correlations.

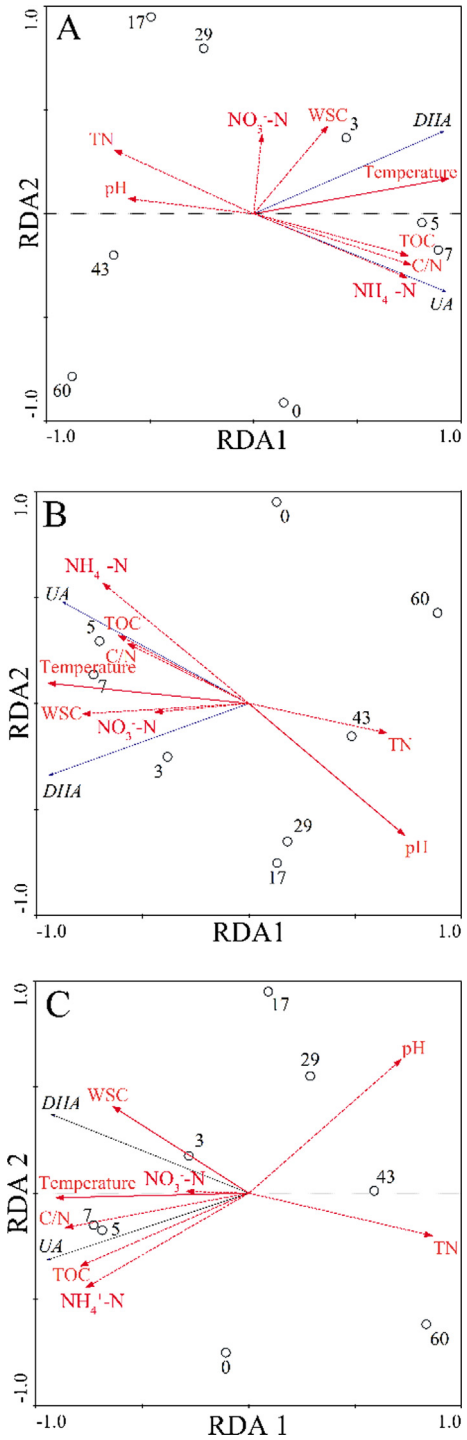

Fig. 4. RDA triplot analysis between enzyme activities and environmental variables. (A) T-C: treatment without Fe_2O_3 NPs or Fe_3O_4 NPs as control; (B) T- Fe_2O_3 NPs: treatment with Fe_2O_3 NPs; (C) T- Fe_3O_4 NPs: treatment with Fe_3O_4 NPs. Significant variables were denoted using red solid lines, and supplementary variables were denoted with red dotted lines. Enzyme activities were presented using black solid lines. The circles indicated samples and the numbers around were the sampling day. (For interpretation of the references to colour in this figure legend, the reader is referred to the web version of this article.)

3.5. Maturity of the final compost product

Generally, C/N ratio is one of the most commonly used indicators to evaluate the rate of composting as well as final compost maturity (Awasthi et al., 2016a). Another important parameter is seed germination index (GI) which is widely used to evaluate the phytotoxicity and maturity of compost, since it directly reflects the effect of compost on the seed germination and seedling growth (Chan et al., 2016). The acceptable final value of C/N for a successful composting is lower than 25 (Chan et al., 2016), and that of GI is above 80% (Wu et al., 2019). As shown in Fig. 5, both C/N and GI met the above requirements, indicating that the end product can be recycled for agricultural application (Chan et al., 2016; Wu et al., 2019). The GI in IONPs treatments, especially that in T-Fe_2O_3 NPs was significant higher than T-C ($P < 0.05$), and the average shoot length in T-C, T-Fe_2O_3 NPs and T-Fe_3O_4 NPs was 3.16, 3.87, 3.45 cm, respectively. This suggested that amendment of IONPs into composting could promote seed germination and seedling growth, a similar finding was reported by Ren et al. (2011) who found that Fe_2O_3 NPs could stimulate the growth of mung bean (*Vigna radiata*).

4. Conclusion

In present study, Fe_2O_3 NPs and Fe_3O_4 NPs were added at a concentration of 10 mg/kg compost to investigate the effects of IONPs on composting performance. With the addition of IONPs especially Fe_2O_3 NPs, the following aspects were changed: (i) the OM degradation was promoted. (ii) DHA and UA were enhanced and the

Table 3
Pearson correlations between enzyme activities and environmental variables.

Treatments	Enzyme activities	Temperature	pH	C/N	TOC	WSC	NH_4^+-N	NO_3^--N	TN
T-C	DHA	0.992**	−0.519	0.557	0.540	0.520	0.583	0.189	−0.550
	UA	0.838**	−0.677	0.732*	0.669	0.337	0.726*	−0.126	−0.707*
T-Fe_2O_3 NPs	DHA	0.953**	−0.591	0.384	0.409	0.827*	0.542	0.420	−0.481
	UA	0.895**	−0.949**	0.498	0.568	0.730*	0.820*	0.253	−0.508
T-Fe_3O_4 NPs	DHA	0.920**	−0.542	0.712*	0.557	0.809*	0.578	0.210	−0.862**
	UA	0.878**	−0.905**	0.771*	0.747*	0.571	0.807*	0.117	−0.700

C/N: total organic carbon/total nitrogen; TOC: total organic carbon; WSC: water soluble carbon; TN: total nitrogen. T-C: treatment without Fe_2O_3 NPs or Fe_3O_4 NPs as control; T- Fe_2O_3 NPs: treatment with Fe_2O_3 NPs; T- Fe_3O_4 NPs: treatment with Fe_3O_4 NPs.
* Correlation is significant at 0.05 level (2-tailed).
** Correlation is significant at 0.01 level (2-tailed).

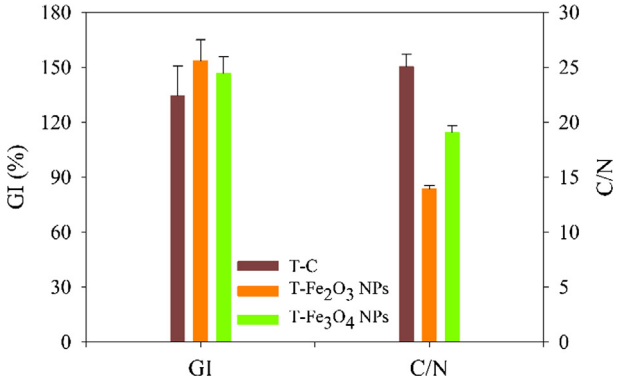

Fig. 5. Maturity indices of the final compost product. GI: germination index; C/N: total organic carbon/total nitrogen. T-C: treatment without Fe_2O_3 NPs or Fe_3O_4 NPs as control; T- Fe_2O_3 NPs: treatment with Fe_2O_3 NPs; T- Fe_3O_4 NPs: treatment with Fe_3O_4 NPs. Mean values were shown and the error bars represented the standard deviations (n = 3).

relationships between enzyme activities and environmental variables were changed. (iii) The seed germination and seedling growth were improved. Therefore, composting amended with IONPs especially Fe_2O_3 NPs is a promising approach to improve the performance of composting process and quality of final compost product.

Acknowledgements

This research was financially supported by the National Natural Science Foundation of China (51521006, 51378190, 51879100, 51408219) and the Program for Changjiang Scholars and Innovative Research Team in University (IRT-13R17).

Appendix A. Supplementary material

Supplementary data to this article can be found online at https://doi.org/10.1016/j.wasman.2019.06.025.

References

Auffan, M., Achouak, W., Rose, J., Roncato, M.A., Chaneac, C., Waite, D.T., Masion, A., Woicik, J.C., Wiesner, M.R., Bottero, J.Y., 2008. Relation between the redox state of iron-based nanoparticles and their cytotoxicity toward *Escherichia coli*. Environ. Sci. Technol. 42, 6730–6735.
Awasthi, M.K., Pandey, A.K., Bundela, P.S., Wong, J.W.C., Li, R.H., Zhang, Z.Q., 2016a. Co-composting of gelatin industry sludge combined with organic fraction of municipal solid waste and poultry waste employing zeolite mixed with enriched nitrifying bacterial consortium. Bioresour. Technol. 213, 181–189.
Awasthi, M.K., Wang, Q., Chen, H.Y., Awasthi, S.K., Wang, M.J., Ren, X.N., Zhao, J.C., Zhang, Z.Q., 2018. Beneficial effect of mixture of additives amendment on enzymatic additives, organic matter degradation and humification during biosolids co-composting. Bioresour. Technol. 247, 138–146.
Awasthi, M.K., Wang, Q., Huang, H., Li, R.H., Shen, F., Lahori, A.H., Wang, P., Guo, D., Guo, Z.Y., Jiang, S.C., Zhang, Z.Q., 2016b. Effect of biochar amendment on greenhouse gas emission and bio-availability of heavy metals during sewage sludge co-composting. J. Clean. Prod. 135, 829–835.
Barton, L.E., Grant, K.E., Kosel, T., Quicksall, A.N., Maurice, P.A., 2011. Size-dependent Pb sorption to nanohematite in the presence and absence of a microbial siderophore. Environ. Sci. Technol. 45, 3231–3237.
Ben-Moshe, T., Frenk, S., Dror, I., Minz, D., Berkowitz, B., 2013. Effects of metal oxide nanoparticles on soil properties. Chemosphere 90, 640–646.
Calvarro, L.M., de Santiago-Martín, A., Gómez, J.Q., González-Huecas, C., Quintana, J. R., Vázquez, A., Lafuente, A.L., Fernández, T.M.R., Vera, R.R., 2014. Biological activity in metal-contaminated calcareous agricultural soils: the role of the organic matter composition and the particle size distribution. Environ. Sci. Pollut. Res. 21, 6176–6187.
Chan, M.T., Selvam, A., Wong, J.W.C., 2016. Reducing nitrogen loss and salinity of 'struvite' food waste composting b zeolite amendment. Bioresour. Technol. 200, 838–844.
Dick, W.A., Cheng, L., Wang, P., 2000. Soil acid and alkaline phosphatase activity as pH adjustment indicators. Soil Biol. Biochem. 32, 1915–1919.
Gitipour, A., El Badawy, A., Arambewela, M., Miller, B., Scheckel, K., Elk, M., Ryu, H., Gomez-Alvarez, V., Domingo, J.S., Thiel, S., Tolaymat, T., 2013. The impact of silver nanoparticles on the composting of municipal solid waste. Environ. Sci. Technol. 47, 14385–14393.
Gong, J.L., Wang, B., Zeng, G.M., Yang, C.P., Niu, C.G., Niu, Q.Y., Zhou, W.J., Liang, Y., 2009. Removal of cationic dyes from aqueous solution using magnetic multi-wall carbon nanotube nanocomposite as adsorbent. J. Hazard. Mat. 164, 1517–1522.
Gutiérrez, I.R., Watanabe, N., Harter, T., 2010. Effect of sulfonamide antibiotics on microbial diversity and activity in a Californian *Mollic Haploxeralf*. J. Soil. Sediment. 10, 537–544.
Hagemann, N., Subdiaga, E., Orsetti, S., de la Rosa, J.M., Knicker, H., Schmidt, H.P., Kappler, A., Behrens, S., 2018. Effect of biochar amendment on compost organic matter composition following aerobic composting of manure. Sci. Total Environ. 613–614, 20–29.
He, K., Chen, G.Q., Zeng, G.M., Chen, A.W., Huang, Z.Z., Shi, J.B., Huang, T.T., Peng, M., Hu, L., 2018a. Three-dimensional graphene supported catalysts for organic dyes degradation. Appl. Catal. B-Environ. 228, 19–28.
He, K., Zeng, Z.T., Chen, A.W., Zeng, G.M., Xiao, R., Xu, P., Huang, Z.Z., Shi, J.B., Hu, L., Chen, G.Q., 2018b. Advancement of Ag-graphene based nanocomposites: An overview on synthesis and its applications. Small 14, 1800871.
He, S.Y., Feng, Y.Z., Ren, H.X., Zhang, Y., Gu, N., Lin, X.G., 2011. The impact of iron oxide magnetic nanoparticles on the soil bacterial community. J. Soil. Sediment. 11, 1408–1417.
He, Z.H., Lin, H., Hao, J.W., Kong, X.S., Tian, K., Bei, Z.L., Tian, X.J., 2018c. Impact of vermiculite on ammonia emissions and organic matter decomposition of food waste during composting. Bioresour. Technol. 263, 548–554.
Huang, Z.Z., He, K., Song, Z.X., Zeng, G.M., Chen, A.W., Yuan, L., Li, H., Hu, L., Guo, Z., Chen, G.Q., 2018. Antioxidative response of *Phanerochaete chrysosporium* against silver nanoparticle-induced toxicity and its potential mechanism. Chemosphere 211, 573–583.
Jurado, M.M., Suárez-Estrella, F., López, M.J., Vargas-García, M.C., López-González, J. A., Moreno, J., 2015. Enhanced turnover of organic matter fractions by microbial stimulation during lignocellulosic waste composting. Bioresour. Technol. 186, 15–24.
Lai, C., Wang, M.M., Zeng, G.M., Liu, Y.G., Huang, D.L., Zhang, C., Wang, R.Z., Xu, P., Cheng, M., Huang, C., Wu, H.P., Qin, L., 2016. Synthesis of surface molecular imprinted TiO_2/graphene photocatalyst and its highly efficient photocatalytic degradation of target pollutant under visible light irradiation. Appl. Surf. Sci. 390, 368–376.
Li, Y.X., Liu, B., Zhang, X.L., Gao, M., Wang, J., 2015. Effects of Cu exposure on enzyme activities and selection for microbial tolerances during swine-manure composting. J. Hazard. Mater. 283, 512–518.
Liu, B., Li, Y.X., Zhang, X.L., Wang, J., Gao, M., 2014. Combined effects of chlortetracycline and dissolved organic matter extracted from pig manure on the functional diversity of soil microbial community. Soil Biol. Biochem. 74, 148–155.
MOA, 2011. National crop straw resources survey and evaluation reports. Agric. Eng. Technol. (Renew. Energy Ind.) 02, 2–5.
NBS CSY (China Statistical Yearbook), 2016. China Statistical Publishing House, Beijing.

Nikaeen, M., Nafez, A.H., Bina, B., Nabavi, B.F., Hassanzadeh, A., 2015. Respiration and enzymatic activities as indicators of stabilization of sewage sludge composting. Waste Manage. 39, 104–110.

Qin, L., Zeng, G.M., Lai, C., Huang, D.L., Xu, P., Zhang, C., Cheng, M., Liu, X.G., Liu, X.Y., Li, B.S., Yi, H., 2018. "Gold Rush" in modern science: Fabrication strategies and typical advanced applications of gold nanoparticles in sensing. Coordin. Chem. Rev. 359, 1–31.

Ren, H.X., Liu, L., Liu, C., He, S.Y., Huang, J., Li, J.L., Zhang, Y., Huang, X.J., Gu, N., 2011. Physiological investigation of magnetic iron oxide nanoparticles towards Chinese mung bean. J. Biomed. Nanotechnol. 7, 677–684.

Ren, L.H., Cai, C.Q., Zhang, J.C., Yang, Y., Wu, G.Y., Luo, L., Huang, H.L., Zhou, Y.Y., Qin, P.F., Yu, M., 2018a. Key environmental factors to variation of ammonia-oxidizing archaea community and potential ammonia oxidation rate during agricultural waste composting. Bioresour. Technol. 270, 278–285.

Ren, X.Y., Zeng, G.M., Tang, L., Wang, J.J., Wan, J., Feng, H.P., Song, B., Huang, C., Tang, X., 2018b. Effect of exogenous carbonaceous materials on the bioavailability of organic pollutants and their ecological risks. Soil Biol. Biochem. 116, 70–81.

Ren, X.Y., Zeng, G.M., Tang, L., Wang, J.J., Wan, J., Liu, Y.N., Yu, J.F., Yi, H., Ye, S.J., Deng, R., 2018c. Sorption, transport and biodegradation-An insight into bioavailability of persistent organic pollutants in soil. Sci. Total Environ. 610–611, 1154–1163.

Stamou, I., Antizar-Ladislao, B., 2016. The impact of silver and titanium dioxide nanoparticles on the in-vessel composting of municipal solid waste. Waste Manage. 56, 71–78.

Sudkolai, S.T., Nourbakhsh, F., 2017. Urease activity as an index for assessing the maturity of cow manure and wheat residue vermicomposts. Waste Manage. 64, 63–66.

Tang, X., Zeng, G.M., Fan, C.Z., Zhou, M., Tang, L., Zhu, J.J., Wan, J., Huang, D.L., Chen, M., Xu, P., Zhang, C., Xiong, W.P., 2018. Chromosomal expression of CadR on *Pseudomonas aeruginosa* for the removal of Cd (II) from aqueous solutions. Sci. Total Environ. 636, 1355–1361.

Wang, K., Li, W., Guo, J., Zou, J., Li, Y., Zhang, L., 2011. Spatial distribution of dynamics characteristic in the intermittent aeration static composting of sewage sludge. Bioresour. Technol. 102, 5528–5532.

Wang, Y.R., Zhu, Y., Hu, Y., Zeng, G.M., Zhang, Y., Zhang, C., Feng, C.L., 2018. How to construct DNA hydrogels for environmental applications: advanced water treatment and environmental analysis. Small 14, 1703305.

Wong, J.W.C., Fang, M., 2000. Effects of lime addition on sewage sludge composting process. Water Res. 34, 3691–13689.

Wu, J., Zhang, A.G., Li, G.X., Wei, Y.Q., He, S.Z., Zhong, L., Shen, X.F., Wang, Q.J., 2019. Effect of different components of single superphosphate on organic matter degradation and maturity during pig manure composting. Sci. Total Environ. 646, 587–594.

Xie, X.F., Pu, L.J., Wang, Q.Q., Zhu, M., Xu, Y., Zhang, M., 2017. Response of soil physicochemical properties and enzyme activities to long-term reclamation of costal saline soil,Eastern China. Sci. Total Environ. 607–608, 1419–1427.

Xiong, W.P., Zeng, Z.T., Li, X., Zeng, G.M., Xiao, R., Yang, Z.H., Zhou, Y.Y., Zhang, C., Cheng, M., Hu, L., Zhou, C.Y., Qin, L., Xu, R., Zhang, Y.R., 2018. Multi-walled carbon nanotube/aminomino-functionalized-53 (Fe) composites: remarkable adsorptive removal of antibiotics from aqueous solutions. Chemosphere 210, 1061–1069.

Xu, P., Zeng, G.M., Huang, D.L., Feng, C.L., Hu, S., Zhao, M.H., Lai, C., Wei, Z., Huang, C., Xie, G.X., Liu, Z.F., 2012. Use of iron oxide nanomaterials in wastewater treatment: A review. Sci. Total Environ. 424, 1–10.

Yang, S.T., Zong, P.F., Ren, X.M., Wang, Q., Wang, X.K., 2012. Rapid and highly efficient preconcentration of Eu (III) by core-shell structured Fe_3O_4@humic acid magnetic nanoparticles. Appl. Mater. Interfaces 4, 6891–6900.

Yang, Y., Zeng, Z.T., Zhang, C., Huang, D.L., Zeng, G.M., Xiao, R., Lai, C., Zhou, C.Y., Guo, H., Xue, W.J., Cheng, M., Wang, W.J., Wang, J.J., 2018a. Construction of iodine vacancy-rich BiOI/Ag@AgI Z-scheme heterojunction photocatalysts for visible-light-driven tetracycline degradation: transformation pathway and mechanism insight. Chem. Eng. J. 349, 808–821.

Yang, Y., Zhang, C., Lai, C., Zeng, G.M., Huang, D.L., Cheng, M., Wang, J.J., Chen, F., Zhou, C.Y., Xiong, W.P., 2018b. BiOX (X = Cl, Br, I) photocatalytic nanomaterials: Applications for fuels and environmental management. Adv. Colloid Interfac. 254, 77–93.

Ye, S.J., Zeng, G.M., Wu, H.P., Zhang, C., Dai, J., Liang, J., Yu, J.F., Ren, X.Y., Yi, H., Cheng, M., Zhang, C., 2017a. Biological technologies for the remediation of co-contaminated soil. Crit. Rev. Biotechnol. 37, 1062–1076.

Ye, S.J., Zeng, G.M., Wu, H.P., Zhang, C., Liang, J., Dai, J., Liu, Z.F., Xiong, W.P., Wan, J., Xu, P., Cheng, M., 2017b. Co-occurrence and interactions of pollutants, and their impacts on soil remediation-A review. Crit. Rev. Env. Sci. Tec. 47, 1528–1553.

Yi, H., Huang, D.L., Qin, L., Zeng, G.M., Lai, C., Cheng, M., Ye, S.J., Song, B., Ren, X.Y., Guo, X.Y., 2018. Selective prepared carbon nanomaterials for advanced photocatalytic application in environmental pollutant treatment and hydrogen production. Appl. Catal. B Environ. 239, 408–424.

Zeng, G.M., Zhang, L.H., Dong, H.R., Chen, Y.N., Zhang, J.C., Zhu, Y., Yuan, Y.J., Xie, Y.K., Fang, W., 2018. Pathway and mechanism of nitrogen transformation during composting: Functional enzymes and genes under different concentrations of PVP-AgNPs. Bioresour. Technol. 253, 112–120.

Zhang, D.F., Luo, W.H., Li, Y., Wang, G.Y., Li, G.X., 2018a. Performance of co-composting sewage sludge and organic fraction of municipal solid waste at different proportions. Bioresour. Technol. 250, 853–885.

Zhang, L.H., Zeng, G.M., Dong, H.R., Chen, Y.N., Zhang, J.C., Yan, M., Zhu, Y., Yuan, Y.J., Xie, Y.K., Huang, Z.Z., 2017. The impact of silver nanoparticles on the co-composting of sewage sludge and agricultural waste: Evolutions of organic matter and nitrogen. Bioesour. Technol. 230, 132–139.

Zhang, L.H., Zeng, G.M., Zhang, J.C., Chen, Y.N., Yu, M., Lu, L.H., Li, H., Zhu, Y., Yuan, Y. J., Huang, A.Z., He, L., 2015. Response of denitrifying genes coding for nitrite (*nirK* or *nirS*) and nitrous oxide (*nosZ*) reductases to different physico-chemical parameters during agricultural waste composting. Appl. Microbiol. Biotechnol. 99 (9), 4059–4070.

Zhang, L.H., Zhang, J.C., Zeng, G.M., Dong, H.R., Chen, Y.N., Huang, C., Zhu, Y., Xu, R., Cheng, Y.J., Hou, K.J., Cao, W.C., Fang, W., 2018b. Multivariate relationships between microbial communities and environmental variables during co-composting of sewage sludge and agricultural waste in the presence of PVP-AgNPs. Bioresour. Technol. 261, 10–18.

Zhou, C.Y., Lai, C., Zhang, C., Zeng, G.M., Huang, D.L., Cheng, M., Hu, L., Xiong, W.P., Chen, M., Wang, J.J., Yang, Y., Jiang, L.B., 2018. Semiconductor/boron nitride composites: synthesis, properties, and photocatalysis application. Appl. Catal. B Environ. 238, 6–18.